



Crystallization study of “melt quenched” amorphous GeTe by transmission electron microscopy for phase change memory applications

A. Bastard, J. C. Bastien, B. Hyot, S. Lhostis, F. Momprou, C. Bonafos, G. Servanton, C. Borowiak, F. Lorut, N. Bicaïs-Lepinay, A. Toffoli, C. Sandhya, A. Fantini, L. Perniola, E. Gourvest, S. Maitrejean, A. Roule, V. Sousa, D. Bensahel, and B. André

Citation: [Applied Physics Letters](#) **99**, 243103 (2011); doi: 10.1063/1.3668095

View online: <http://dx.doi.org/10.1063/1.3668095>

View Table of Contents: <http://scitation.aip.org/content/aip/journal/apl/99/24?ver=pdfcov>

Published by the [AIP Publishing](#)



Re-register for Table of Content Alerts

Create a profile.



Sign up today!



Crystallization study of “melt quenched” amorphous GeTe by transmission electron microscopy for phase change memory applications

A. Bastard,^{1,2,3,a)} J. C. Bastien,^{2,4} B. Hyot,² S. Lhostis,^{1,2} F. Momprou,³ C. Bonafos,³ G. Servanton,¹ C. Borowiak,¹ F. Lort,¹ N. Bicais-Lepinay,¹ A. Toffoli,² C. Sandhya,² A. Fantini,² L. Perniola,² E. Gourvest,^{1,2} S. Maitrejean,² A. Roule,² V. Sousa,² D. Bensahel,¹ and B. André²

¹ST Microelectronics, 850 Rue Jean Monnet, 38920 Crolles, France

²CEA-LETI, MINATEC Campus, 17 rue des Martyrs, 38054 Grenoble Cedex 9, France

³CEMES-CNRS, Université de Toulouse, 29 rue Jeanne Marvig, BP 94347, 31055 Toulouse Cedex 4, France

⁴Laboratoire Verres et Céramiques, Sciences Chimiques de Rennes-UMR CNRS 6226, Campus de Beaulieu, 35052 Rennes Cedex, France

(Received 27 September 2011; accepted 18 November 2011; published online 12 December 2011)

In situ transmission electron microscopy (TEM) observations were performed for a better understanding of the “melt quenched” GeTe crystallization mechanism. The evolution of the crystallite morphology observed during annealing shows a growth-dominated crystallization behavior. Scanning transmission electron microscopy—electron dispersive x-ray spectroscopy and high resolution electron microscopy experiments were also performed on cycled GeTe devices, showing that void formation is responsible for the cell failure after 10⁷ cycles. © 2011 American Institute of Physics. [doi:10.1063/1.3668095]

Phase change material (PCM) studies are mostly based on the investigation of the “as-deposited” amorphous material crystallization.^{1–5} Few publications focus on the closest form of amorphous material in the final devices, the so-called “melt quenched”^{6,7} form. The study of this amorphous phase is made difficult since it requires the amorphization of the material followed by the study of the “melt-quenched” spot with a nanometric spatial resolution. However, it is of prime importance to analyze this “melt-quenched” amorphized material, as it presents different properties from the “as-deposited” material^{8,9} and because the crystallization mechanism of phase change materials that occurs during the functioning of the memory is of great relevance. The crystallization proceeds following two types of mechanisms:^{10,11} (1) crystallization by nucleation that takes place both in the interior and at the edges of the spot and (2) recrystallization by growth that only happens by propagation from the crystalline amorphous boundary. These two types of behavior may or may not be advantageous, depending on whether nucleation is desirable (the seeded nuclei can accelerate crystallization) or not (faster lost of data at low temperatures).

The aim of this work is first to demonstrate the nature of the crystallization mechanism of “melt quenched” amorphous GeTe by *in situ* transmission electron microscopy (TEM). Thereafter, the crystallization behavior of the material, integrated into a device, has been investigated following several cycles.

The GeTe material was deposited using DC magnetron sputtering from an elemental GeTe target. The composition was checked by Rutherford back scattering spectrometry (RBS). A 100 nm thick film was deposited on an insulator/phase change material/insulator/metal (IPIM) structure that allows the subsequent amorphization of the sample. The

samples were then annealed under vacuum at 400 °C, after which, a series of amorphous spots was introduced in the previously crystallized material by laser annealing. During this process, the samples were exposed to laser pulses at a preset power (70 mW) and duration (160 ns) using a pulsed laser with a wavelength of 504 nm.

The samples were then prepared for *in situ* TEM observations by mechanical polishing and ion milling under N₂ cooling. The *in situ* TEM observations were carried out using a JEOL 2010 operating at 200 kV equipped with a Gatan heating holder and a temperature controller. Video sequences were recorded with a Megaview III camera at 25 frames per seconds. The samples were first heated to 100 °C at the maximum heating rate. They were subsequently heated above 100 °C at a rate of 10 °C/min. The temperature was then kept constant above the crystallization temperature (180 °C).

Afterwards, the material was integrated into devices which were submitted to programming tests¹² under reset/set pulses and prepared by focus ion beam using Ga ion milling. These samples were observed with a Tecnai Osiris TEM operating at 120 kV dedicated to scanning transmission electron microscopy—electron dispersive x-ray spectroscopy (STEM-EDS) analysis. Finally, high resolution electron microscopy (HREM) observations of these samples were made with a FEI Tecnai microscope equipped with a field emission gun and a spherical aberration corrector, operating at 200 kV.

Figure 1 illustrates the crystallization of the “melt quenched” amorphous GeTe during an *in situ* TEM experiment. The four images have been extracted from a video sequence at multiple time intervals in order to give an overview of the whole crystallization process at 155 °C. The amorphous spot is initially surrounded by the crystalline GeTe material (Fig. 1(a)). The average spot size is 366 nm with a statistical distribution of 28 nm. Note that the initial

^{a)}Author to whom correspondence should be addressed. Electronic mail: audreybas@free.fr.

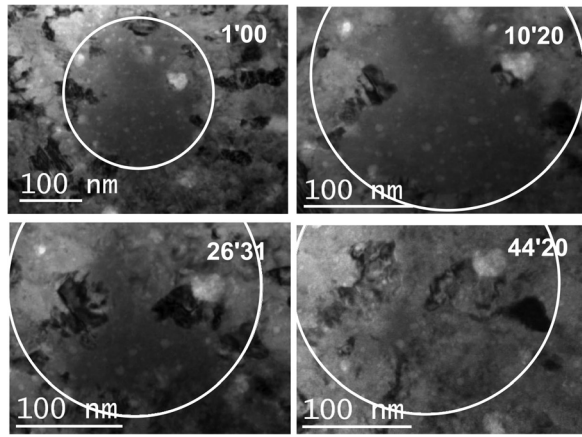


FIG. 1. TEM bright field images selected from the *in situ* crystallization sequence of the GeTe “melt quenched” spot at 155 °C.

size of the spot is represented by a white circle in Figure 1. We observe that, during the isothermal annealing, some grains from the crystalline matrix grow unequally. We also note the absence of crystalline nuclei formation inside the amorphous spot (Figs. 1(b) and 1(c)). After completion of the crystallization process, the amorphous spot is barely distinguishable from the crystalline background (Fig. 1(d)). From these observations, using our annealing conditions and sample preparation, we can conclude that GeTe has a growth-dominated crystallization mechanism. In the literature, there is no consensus regarding the crystallization behavior of GeTe. Some results have shown that the compositions are playing an important role in the crystallization mechanism of GeTe.^{13,14} The sample preparation, thinner for TEM characterization and thicker for a static tester stack, can also disturb this mechanism. However, in our case, for thin Ge₅₃Te₄₇ crystallized by thermal annealing, the video sequence shows a crystallization mechanism dominated by growth.

Recently, Gawelda *et al.*¹⁵ have studied both the amorphous and crystalline transformations of GeTe under femto and nanosecond irradiation. Although their experiment was not performed in the same conditions as ours, they demonstrated a growth based crystallization behavior during the first few irradiating pulses of the melt quench. With further pulses, they observed a nucleation mechanism that became dominant until complete crystallization was achieved.

In our work, the crystallization of the “melt quenched” spots has been studied at three different temperatures (120, 140, and 155 °C). This allowed us to determine the growth rate, u , of the grains by measuring the average crystallite size at each temperature before impingement with neighboring crystallites.

For multiple grains, we measured several different growth rates of 4 ± 3 pm/s, 32 ± 15 pm/s, and 132 ± 40 pm/s at 120, 140, and 155 °C, respectively. The large error bars result from the difficulty in measuring the grain size.

“As-deposited” materials were investigated by Wuttig and Steimer.¹⁶ They followed the varying number and size of crystals during the crystallization process using AFM measurements. They reported growth rates ranging from 7 pm/s to 60 nm/s for materials such as AgInSb₂Te, Ge₂Sb₂Te₅, and Ge₄Sb₁Te₅. These growth rates are comparable to those measured in our work.

From our measured values, we can plot the Arrhenius law characteristics of the grain growth:¹⁷

$$\ln(u) = -\frac{E_u}{k_B T} + C, \quad (1)$$

where E_u is the activation energy for growth, k_B the Boltzmann constant, and C a constant. These data are shown in Figure 2. From the slope, we obtain the activation energy for growth which is 1.45 ± 0.38 eV (Fig. 2). We can reasonably assume a temperature uncertainty of ± 5 °C with respect to the temperature controller setting. In addition, the electron beam is known to affect the crystallization process due to local heating⁷ so we also assume that the temperature inside the material is higher than that stated. The value of E_u obtained above is, therefore, an underestimation of the real activation energy.

Previously, only one value of the activation energy for GeTe growth has been reported in the literature.¹⁸ This study focused on the crystallization mechanism of the “as-deposited” material and a value of $E_u = 1.77 \pm 0.14$ eV was measured, which is, taking into account the error bars, close to our measurement.

This study has given us a better understanding of the GeTe crystallisation mechanism but this raises questions as to how the material behaves following repeated amorphization/crystallization cycles. Thus, we performed endurance measurements via programming tests on GeTe for up to 10⁷ cycles. The STEM-EDS maps of the same GeTe device after one step of “melt quenched” amorphization and after 10⁷ cycles of “melt quenched” amorphization/crystallization are shown in Figs. 3(a) and 3(b), respectively. The element composition of the device is represented using different colors. In the second image (Fig. 3(b)), we note the presence of voids at the PCM/heater interface which is attributed to the damage caused by successive cycles. No segregation of Ge or Te elements was observed in the EDS profile. Additional HREM observations of these cycled devices showed that thinner regions appear at the interface with the heater (Fig. 3(c)). This is confirmed by thickness mapping performed in electron energy loss spectroscopy (EELS). Such void formation after cycling is currently observed in other cycled devices^{19,20} and is shown to be due to material stress at the interface with the heater. Thus, the potential origin of the device failure may be due to density variation of the material during successive cycles.

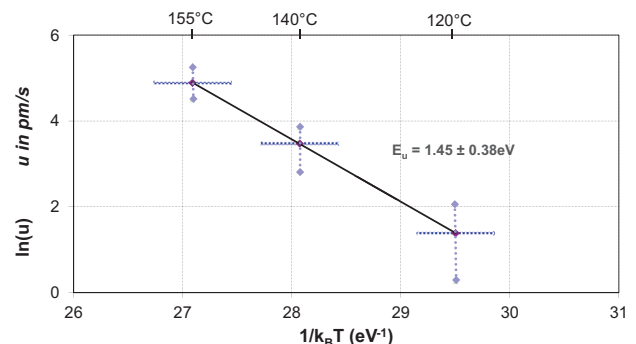


FIG. 2. (Color online) Activation energy for growth extracted from the slope of the Arrhenius plot (Eq. (1)) dotted lines represent error bars.

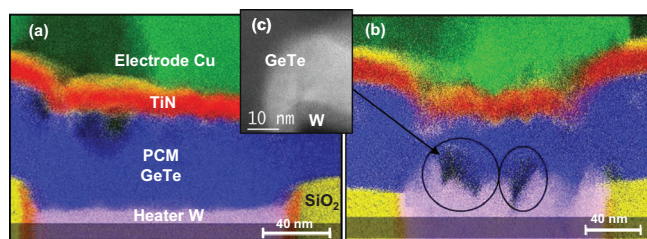


FIG. 3. (Color online) STEM-EDS maps of GeTe devices after (a) one amorphization and (b) after 10^7 cycles. Contrast colors correspond to the different elements of the device. (c) HREM image taken of the dark region encircled in (b).

In conclusion, we have demonstrated, using *in situ* TEM observations, that the crystallization mechanism of “melt quenched” GeTe is dominated by growth from the crystalline/amorphous boundary. The study of cycled devices shows that the failure may be due to a change of density during cycling, which eventually leads to voids formation.

The *in situ* TEM observations were performed within the METSA network.

¹E. T. Kim, J. Y. Lee, and Y. T. Kim, *Phys. Status Solidi A* **206**(11), 2542 (2009).

²Y. S. Hsu, Y.-D. Liu, Y.-C. Her, S.-T. Cheng, and S.-Y. Tsai, *Jpn. J. Appl. Phys.* **47**(7) 6016 (2008).

³S. Raoux, C. Cabral, Jr., L. Krusin-Elbaum, J. L. Jordan-Sweet, K. Viv-rwani, M. Hitzbleck, M. Salinga, A. Madan, and T. L. Pinto, *J. Appl. Phys.* **105**, 064918 (2009).

⁴Y. Zhang, J. Feng, and B. Cai, *Appl. Surf. Sci.* **256**(7) 2223 (2010).

⁵Y.-G. Yoo, D.-S. Yang, H. J. Ryu, W. S. Cheong, and M. C. Baek, *Mater. Sci. Eng. A* **449–451** 627 (2007).

⁶R. M. Shelby and S. Raoux, *J. Appl. Phys.* **105**, 104902 (2009).

⁷B. J. Kooi, W. M. G. Groot, and J. Th. M. De Hosson, *J. Appl. Phys.* **95**(3), 924 (2004).

⁸S. Raoux, H.-Y. Cheng, M. A. Caldwell, and H.-S. P. Wong, *Appl. Phys. Lett.* **95**, 071910 (2009).

⁹A. Kolobov, *Nature Mater.* **7**, 351 (2008).

¹⁰G. F. Zhou, H. J. Borg, J. C. N. Rijpers, M. H. R. Lankhorst, and J. J. L. Horikx, *Optical Data Storage, 2000. Conference Digest* (2000), pp. 74–76, DOI: 10.1109/ODS.2000.847985.

¹¹Y. H. Shih, J. Y. Wu, B. Rajendran, M. H. Lee, R. Cheek, M. Lamorey, M. Breitwisch, Y. Zhu, E. K. Lai, C. F. Chen *et al.*, *Tech. Dig. - Int. Electron Devices Meet.* **2008**, 207.

¹²L. Perniola, V. Sousa, A. Fantini, E. Arbaoui, A. Bastard, M. Armand, A. Fargeix, C. Jahan, J.-F. Nodin, A. Persico *et al.*, *IEEE Electron Device Lett.* **31**(5), 488 (2010).

¹³M. Libera and M. Chen, *J. Appl. Phys.* **73**(5), 2272 (1993).

¹⁴J. H. Coombs, A. P. J. M. Jongenelis, W. van Es-Spiekman, and B. A. J. Jacobs, *J. Appl. Phys.* **78**, 4906 (1995).

¹⁵W. Gawelda, J. Siegel, C. N. Afonso, V. Plaisinaitiene, A. Abrutis, and C. Wiemer, *J. Appl. Phys.* **109**, 123102 (2011).

¹⁶M. Wuttig and C. Steimer, *Appl. Phys. A* **87**, 411 (2007).

¹⁷J. Kalb, F. Spaepen, and M. Wuttig, *Appl. Phys. Lett.* **84**, 5240 (2004).

¹⁸Q. M. Lu and M. Libera, *J. Appl. Phys.* **77**(2), 1 (1995).

¹⁹K. Kim and S. J. Ahn, in *IEEE International Reliability Physics Symposium Tech. Dig.* (IEEE, New York, 2005), pp. 157–162.

²⁰B. Gleixner, F. Pellizzer, and R. Bez, *Proceeding of ePCOS*, pp. 135–139, Sep. 2009.